Journal of Science and Technology – Engineering and Technology for Sustainable Development
Volume 35, Issue 5, November 2025, 043-049

Study on the Conversion of PCB-138 (2,2',3,4,4',5'-Hexachlorobiphenyl) via Hydrodechlorination Reaction Using Fe/Cu and Fe/Ni Bimetallic Nanocatalysts

Hong Son Nguyen[1], Van Hoang Nguyen[1], Thanh Hung Nguyen[2], Ngoc Toan Vu[1*],
[1]Institute of New Technology, Ha Noi, Vietnam
[2]Hanoi University of Science and Technology, Ha Noi, Vietnam
[*]Corresponding author email: vntoanchem@gmail.com

Abstract

Research on PCB-138 treatment is always urgent, along the development of nanotechnology has created general conditions to apply them in this treatment process. With low cost and easy synthesis of Fe/Cu and Fe/Ni bimetallic nanoparticles, the hydrodechlorination (HDC) reaction was conducted to convert PCB-138 in aqueous media into non-toxic or less toxic products. The study results revealed that the optimal conditions for achieving high PCB-138 conversion efficiency were: [Fe/Cu] = 2,0 g/L, pH = 3; [Fe/Ni] = 2,0 g/L, pH = 7, with a reaction time of 120 to 180 min required to reach adsorption equilibrium. Experimental data indicated that the adsorption of PCB-138 followed a pseudo-second-order kinetic model, confirming a chemisorption mechanism on the surface of the catalytic nanoparticles. Furthermore, the conversion pathway of PCB-138 was proposed, involving the formation of less toxic products such as biphenyl, thereby demonstrating the efficacy of the HDC reaction. This study highlights the practical potential of bimetallic nanoparticles in treating water contaminated with chlorinated organic compounds.

Keywords: Fe/Cu, Fe/Ni, hydrodechlorination, PCB-138.

1. Introduction

In recent years, Fe^0-based bimetallic nanoparticles (BNPs-Fe^0) have garnered significant attention from the scientific community due to their outstanding advantages, including large surface area, strong catalytic capability, and superior efficiency in treating pollutants compared to monometallic nanoparticles [1]. Notably, the incorporation of a second transition metal, such as Ni, Cu, or Pd, to enhance the catalytic activity of BNPs-Fe^0, has been well-documented in numerous studies [2]. In the Fe/Cu bimetallic system, the electrochemical potential difference between Fe ($E_{Fe^{2+}/Fe}$ = -0.44 V) and Cu ($E_{Cu^{2+}/Cu}$ = +0.34 V) generates a natural electron flow from Fe to Cu when the two metals are in direct contact. This electrochemical interaction significantly improves the catalytic performance of the nanoparticles. Similarly, the inclusion of Ni in BNPs-Fe^0 has been shown to further enhance their catalytic capabilities, promoting the reduction of pollutants such as dyes, chlorinated organic compounds, nitrates, heavy metals, and antibiotics [3]. These findings underscore the immense potential of BNPs-Fe^0 as an advanced technological solution in the field of environmental protection.

Polychlorinated biphenyls (PCBs) are a group of aromatic chlorinated organic compounds comprising 209 congeners with the molecular formula $C_{12}H_{(10-n)}C1_n$ ($1 \leq n \leq 10$). These compounds are characterized by their high toxicity and remarkable environmental persistence. Although the production of PCBs has been prohibited in the United States since 1978 and is restricted under the Stockholm Convention of 2001, they remain in use in certain electrical equipment as dielectric fluids or as contaminants within these fluids. This ongoing usage poses significant environmental risks, particularly in mining areas near groundwater sources. When PCBs leak or are released from improperly disposed of equipment, they can migrate into groundwater, leading to severe contamination that is challenging to remediate. Umasangaji *et al*. [4] reported that nearly 40% of benthic aquatic ecosystems have been at a high risk of PCB contamination, based on data collected over the past three decades. Given that the LD50 of PCBs is between 1-10 g/kg [5], the persistence and toxicity of these contaminants pose significant environmental and ecological threats. In recent years, metallic nanoparticles have been extensively studied and applied as advanced materials for PCBs remediation. The surface-catalyzed hydrodechlorination (HDC) of chlorobenzene is generally proposed to proceed via the mechanism illustrated in Fig. 1 [8]. Studies by Zhen Zhang (2012) [6], and Gil-Diaz (2022) [7] have demonstrated the efficiency and potential

p-ISSN 3093-3242
e-ISSN 3093-3579
https://doi.org/10.51316/jst.186.etsd.2025.35.5.6
Received: Feb 7, 2025; Revised: Jun 13, 2025
Accepted: Jul 17, 2025; Online: Oct 20, 2025.

of using these materials, including BNPs-Fe^0 for PCB degradation. Operating through the hydrodechlorination (HDC) mechanism, BNPs-Fe^0 can cleave C-Cl bonds, releasing Cl^- ions via the following reaction:

$$2Fe^0 + R\text{-}Cl + 3H_2O \rightarrow 2Fe^{2+} + R\text{-}H + 3OH^- + H_2 + Cl^- \quad (1)$$

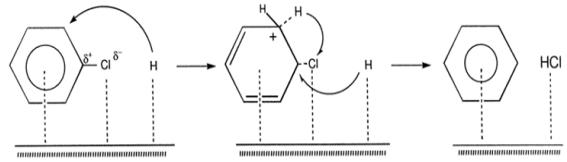

Fig. 1. Proposed reaction scheme for the surface-catalyzed HDC of chlorobenzene

In this study, the remediation and transformation capability of PCB-138 in aqueous media was evaluated through a catalytic dechlorination reaction using BNPs Fe/Ni and Fe/Cu bimetallic nano catalysts. These materials were synthesized via a green method, following the procedure previously reported by our research group [9], in which green tea extract was employed as a natural reducing and stabilizing agent. Unlike previous studies using chemically synthesized Fe^0-based materials, this approach offers a more environmentally friendly alternative while maintaining high catalytic efficiency. Based on the analytical results obtained from gas chromatography-mass spectrometry (GC/MS), a transformation pathway for PCB-138 was proposed, encompassing intermediate stages and final products.

2. Experiment and Method

2.1. Chemical

BNPs Fe/Cu and Fe/Ni bimetallic nanocatalysts were synthesized using a green method based on the procedure established in our earlier work, and some basic properties of these two materials are presented in this study; PCB-138 (99.5 %, EhrenStorfer, UK); *n*-hexane (99 %, Fisher Chemical, USA); Dichloromethane (99.8 %, Fisher Chemical, USA); sodium sulfate (99 %, Xilong Scientific, China); RO water (Milli-Q, Merck Millipore, France) and some other common chemicals.

2.2. Experimental Conversion of PCB-138

2.2.1. Effect of BNPs content and type

The experiment was carried out by Environmental Protection Agency (EPA) Method 8082A. A range of BNPs (Fe/Cu, Fe/Ni) and nano zero-valent iron (nZVI) at concentrations between 0.4 g/L and 2.4 g/L were evaluated. These nanoparticles were introduced into 50 mL of water spiked with 100 µg/L of PCB-138 in conical flasks, followed by stirring at ambient temperature. The reaction mixture underwent triple extraction with 10 mL of dichloromethane and was subsequently treated with 3-5 g of anhydrous Na_2SO_4. After allowing the mixture to stand for 10 min, the solution was transferred to a single-neck flask, combined with 10 mL of *n*-hexane, and concentrated under vacuum to a final volume of 1-2 mL. The resulting solution was filtered through a 0.22 µm membrane (Newstart, China), transferred to a 2 mL vial, and analyzed using a GC/MS system (Agilent 5975C, USA) with a 1 µL injection volume. The GC/MS conditions for PCB-138 analysis were configured as follows (Table 1).

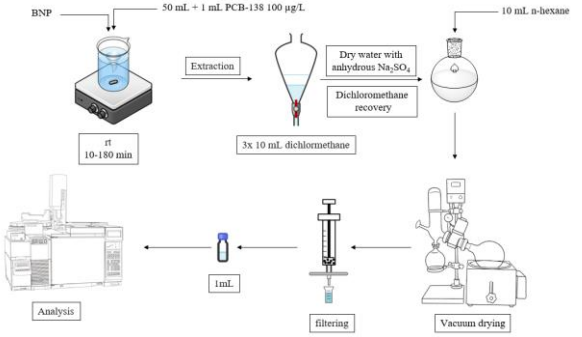

Fig. 2. Sample preparation and analysis procedures

Table 1. Gas chromatography and analysis program

GC –Gas Chromatography	Information
Chromatographic column	DB-5MS UI (30 m ×0.250 mm × 0.25 µm)
Carrier gas flow (He)	20 mL/min
Injector temperature	200 °C
Detector temperature	290 °C
Initial temperature	100 °C hold for 2 min
Temperature program	100 °C - 160 °C, heating rate 15 °C/min, 160 °C - 270 °C, heating rate 5 °C/min
Final Temperature	270 °C
Inlet Sample injection volume	1 µL
Total running time	28 min

2.2.2. Effect of pH

The experimental procedure was conducted in a manner consistent with the previous description. The water *pH* at 2, 3, 5, 7, and 9 values were adjusted using 0.1 M H_2SO_4 and 0.1 M NaOH solutions. The investigation did not include higher *pH* environments due to the significant impact of hydroxide formation on the properties of BNPs-Fe^0 [8, 9]. The *pH* that yielded the highest PCB-138 conversion efficiency will be selected for the subsequent investigations. Additionally, the point of zero charge (pH_{pzc}) of BNPs-Fe^0 was

determined using the method described by Balistrieri and Murray [10]. This approach involves plotting the relationship between *pH* and *ΔpH*. The intersection point of the *ΔpH* curve with the initial *pH* (pH_i) represents the pH_{pzc} value of the BNPs-Fe^0.

2.2.3. Effect of reaction time

The conversion of PCB-138 was examined at various reaction times ranging from 10 to 180 min using the same procedure mentioned earlier. The experiments were conducted three times, and the average values were calculated.

2.3. PCB-138 Metabolic Pathway

To determine the retention time of PCB-138, the high-concentration sample was analyzed in SCAN mode, which involved conducting a full scan at m/z 50-650. For the low-concentration post-treatment sample, the MS was used in SIM mode to focus on biphenyl and metabolic intermediates with lower C-Cl bond numbers than the original PCB-138. The study by Osemwengie *et al.* (2013), on which our methodology is based, provides the referenced m/z values for these compounds [11]. The identification of intermediate products in the transformation process was conducted by matching the m/z fragments with the NIST spectral library.

2.4. Examining the BNPs Reusability

The BNPs-Fe^0 after the HDC reaction were regenerated by filtration and drying under an inert atmosphere (N_2). The changes in their morphology and surface features were investigated using SEM analysis (Jeol Neoscope JCM-7000, Japan). The BNPs-Fe^0 was tested for reusability over 5 cycles.

3. Results and Discussion

3.1. Factors Influencing the HDC Reaction of PCB-138

3.3.1. Effect of BNPs-Fe^0 content and type

The results of the study on the effect of BNPs-Fe^0 content and type on the conversion efficiency of PCB-138 are presented in Fig. 3.

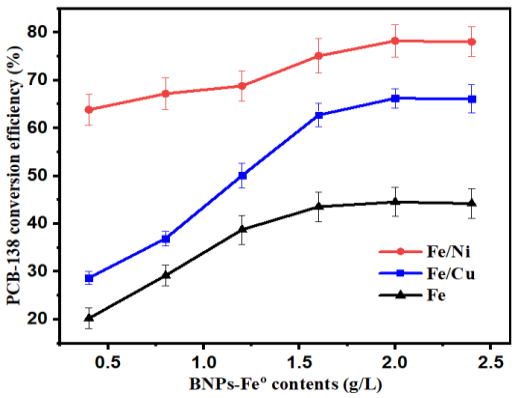

Fig. 3. Effect of BNPs-Fe^0 content and type on PCB-138 conversion efficiency

The conversion of PCB-138 increased progressively as the BNPs concentration was raised from 0.4 g/L to 1.6 g/L, with little to no change observed upon further increase from 1.6 g/L to 2.4 g/L. The highest conversion efficiency of PCB-138 was achieved at 66.24 % and 78.24 %, corresponding to concentrations of 2.0 g/L for the Fe/Cu and Fe/Ni systems, respectively.

The highest conversion efficiency of 44.50 % was observed when using Fe^0 nanoparticles alone as the catalyst. This indicates that the addition of a second metal can enhance and promote the conversion efficiency of PCB-138 through synergistic effects. The difference in dechlorination performance of PCB-138 when using the two types of BNPs-Fe^0 catalysts could be attributed to the distinct adsorption behaviors of PCB-138 molecules on the surfaces of these materials. The magnetic properties of Fe/Ni may generate a stronger magnetic environment [12], facilitating the adsorption and rearrangement of molecules, which in turn accelerates the adsorption process due to a stronger interaction between the PCB-138 molecules and the catalyst surface. Additionally, Cu nanoparticles are highly sensitive to air and tend to oxidize upon exposure to atmospheric oxygen [13] even with a protective polyphenol coating. This may contribute to the observed differences in adsorption capacity between the Fe/Ni and Fe/Cu systems. While Fe/Cu nanoparticles may undergo oxidation and aggregation upon contact with air, Fe/Ni nanoparticles appear to be less sensitive to these phenomena. These findings are consistent with previous studies, such as those by Venkateshaiah *et al.* (2022) [14].

3.3.2. Effect of pH

The results shown in Fig. 4a) indicate that the conversion efficiency of PCB-138 is significantly dependent on the *pH* of the reaction environment. Specifically, when Fe/Cu is used as the catalyst, the highest conversion efficiency of 73.59 % is achieved at *pH* value of 3, with a gradual decrease as the *pH* increases. In contrast, Fe/Ni exhibits the highest efficiency of 78.24 % at *pH* equal 7. This phenomenon may be related to the stability of the nanoparticles and the surface interactions between the catalyst and PCB-138 at different *pH* levels. Fig. 4b) provides information on the point of zero charge pH_{pzc} of Fe/Cu and Fe/Ni, with values of 3.51 and 7.46, respectively. At *pH* values lower than the pH_{pzc}, the material surface carries a positive charge, facilitating the adsorption of PCB-138. This explains why Fe/Cu exhibits the highest efficiency in the *pH* range of 3-4, where the catalyst surface is positively charged, optimizing interactions with PCB-138. In contrast, at *pH* values greater than the pH_{pzc}, the material surface becomes negatively charged, reducing interactions with PCB-138, and leading to lower treatment efficiency. Similarly, for Fe/Ni, with a pH_{pzc} of 7.64, the material surface carries a neutral or slightly positive charge, enabling Fe/Ni to perform optimally under these conditions.

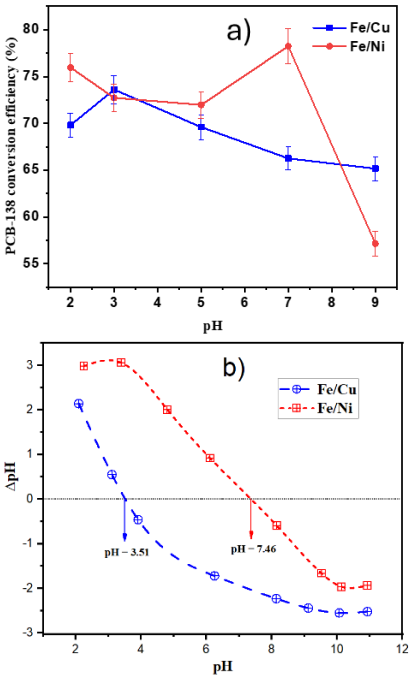

Fig. 4. a) Effect of pH on PCB-138 metabolism; b) Graph to determine the isoelectric point of BNPs

Patanjali *et al.* [15] suggested that decreasing the *pH* from neutral to slightly acidic does not significantly affect the PCB degradation process, as the environment already provides sufficient protons for the reaction. Furthermore, Zhao *et al.* [16] indicated that an initial *pH* of 5.41 is optimal for the degradation of PCB-78. In a study by Sun *et al*. [17], the highest removal rate for PCB-67 in soil was achieved at *pH* equal 3.5. These studies collectively suggest that the optimal *pH* for PCB degradation may vary, depending on different factors such as the type of PCB congener, the catalyst used, and the reaction conditions, indicating that *pH* optimization is a complex process influenced by multiple variables.

3.3.3. Effect of time reaction

The results of the investigation on the effect of reaction time between BNPs (Fe-Cu, Fe/Ni) and PCB-138 are shown in Fig. 5. The findings indicate that the conversion efficiency of PCB-138 tends to increase gradually as the reaction time is extended. The graph illustrates that the conversion efficiency of PCB-138 increases with the reaction time, stabilizing after approximately 120 min. The maximum conversion efficiency was achieved using Fe/Cu catalyst, reaching 75.70 % ([PCB-138] = 50 µg/L, t = 180 min) and 68.08 % ([PCB-138] = 100 µg/L, t = 120 min). In contrast, with BNPs Fe/Ni, the highest conversion efficiencies were 75.85 % ([PCB-138] = 50 µg/L, t = 180 min) and 72.39 % ([PCB-138] = 100 µg/L, t = 180 min). Based on these results, a kinetic model was developed to further assess the adsorption process of PCBs by BNPs.

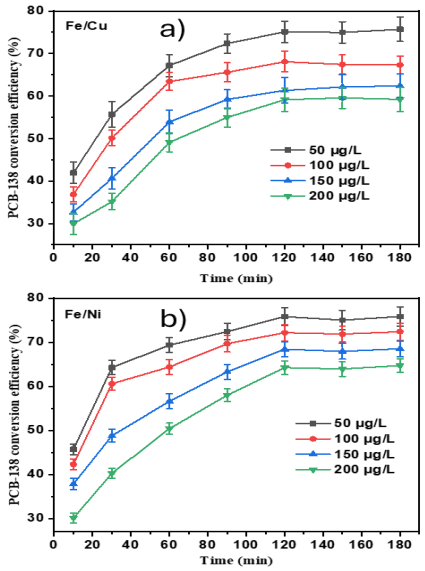

Fig. 5. Effect of reaction time with BNPs catalysts a) Fe/Cu, b) Fe/Ni on the conversion efficiency of PCB-138 in water

Xiuqin *et al*. [18] demonstrated a removal efficiency of 71.94% for a PCB mixture within 6 h. Similarly, surface-modified nZVI reported by Gomes *et al*. [19] exhibited PCB removal efficiencies ranging from 9% to 96%, with PCB-138 achieving the highest removal rate. These findings highlight the potential of Fe/Cu and Fe/Ni BNPs in this study as effective materials for PCB-138 remediation, with competitive or superior performance under optimized conditions. This suggests that bimetallic nanoparticles synthesized in this work are promising candidates for further development in PCB degradation applications.

3.2. Reaction Kinetics

The experimental data in the first-order and second-order kinetic models for the conversion of PCB-138 are presented in Table 2.

The kinetic parameters presented in Table 2 indicate that the pseudo-second-order model fits the PCB-138 reduction process more accurately than the pseudo-first-order model, as reflected by higher R^2 values in most cases. Specifically, for the Fe/Cu catalyst, R^2 values from the pseudo-second-order model ranged from 0.8353 to 0.8819, compared to 0.7230 to 0.8580 for the first-order model. Similarly, for Fe/Ni, the pseudo-second-order model yielded R^2 values of 0.8291-0.9214, consistently higher than those of the first-order model (0.7560-0.8980). These results suggest that the reaction rate is not solely dependent on PCB-138 concentration in solution, but also on the availability of active sites on the catalyst surface, typical of surface-mediated heterogeneous reactions involving adsorption steps.

Table 2. Kinetic reaction parameters of PCB-138, calculated based on theory and experiment

Parameters	Fe/Cu				Fe/Ni			
	PCB-138 concentration (µg/L)				PCB-138 concentration (µg/L)			
	50	100	150	200	50	100	150	200
First-order								
k_1 (min^{-1})	0.0049	0.0036	0.0034	0.0034	0.0041	0.0038	0.0040	0.0041
$t_{1/2}$ (min)	141.4	192.5	203.8	203.8	169.0	182.4	173.3	169.0
R^2	0.8257	0.7230	0.8352	0.8580	0.7560	0.7676	0.8802	0.8980
Second-order								
k_2 ($min^{-1}µg^{-1}L^{-1}$)	3×10^{-4}	1×10^{-4}	5×10^{-5}	3×10^{-5}	2×10^{-4}	1×10^{-4}	6×10^{-5}	4×10^{-5}
$t_{1/2}$	66.7	100.0	133.3	166.7	100.0	100.0	111.1	125.0
R^2	0.8781	0.8353	0.8686	0.8819	0.8291	0.8854	0.075	0.9214

3.3. PCB-138 Conversion Process

The reduction in PCB-138 concentration in water after the HDC reaction using BNPs catalysts (Fe/Cu and Fe/Ni) is shown in the chromatograms in Fig. 6. The results from the chromatograms indicate that after the reaction, the transformation of PCB-138 is evident, as reflected by the change in peak height and area within the retention time range of 22.762-22.773 min. In the HyperChem model, the C-Cl bond length at position 3 meta position) reaches a maximum value of 1,7468 Å.

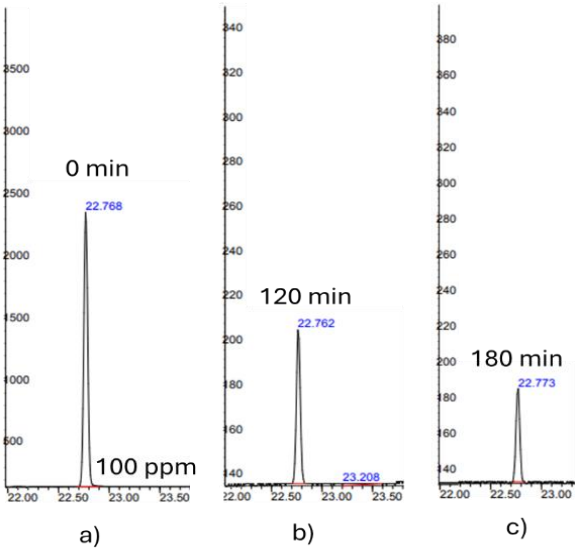

Fig. 6. Chromatograms a) PCB-138 (n-hexane) 100 µg/L; b) After treatment with [Fe/Cu] equal 2.0 g/L, *pH* equal 3, *t* equal 120 min; c) After treatment with [Fe/Ni] equal 2.0 g/L, *pH* equal 7, *t* equal 180 min

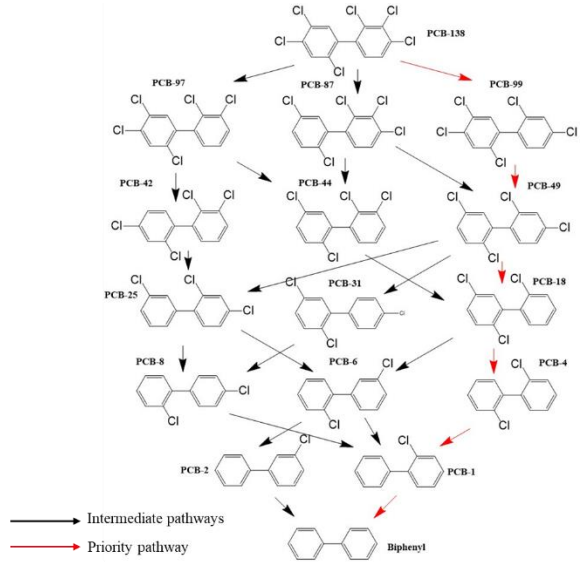

Fig. 7. Possible dechlorination pathways of PCB-138 in the aquatic environment

The C-Cl bond at this position is more polarized compared to other positions due to the significant charge difference between the chlorine and carbon atoms. Additionally, chlorine atoms at the ortho-position (directly bonded on the ring) are generally more resistant to substitution due to spatial shielding effects and steric hindrance. In contrast, chlorine at the para and meta positions is typically easier to replace in certain reactions. Several studies have shown that chlorine atoms at the *para* and *meta* positions are more susceptible to nucleophilic substitution than those at the *ortho* position, owing to both electronic and steric factors [20]. Based on the analysis results and the NIST

library spectra, the transformation pathway leading to the formation of intermediate products for PCB-138 interacting with BNPs is proposed in Fig. 7, with the preferred transformation pathway being **PCB-138 → PCB-99 → PCB-49 → PCB-18 → PCB-4 → PCB-1 → Biphenyl.**

3.4. BNPs-Fe^0 Reusability

Reusing BNPs while maintaining their efficiency offers a practical approach to reducing synthesis expenses and minimizing solvent waste. Additionally, the ability of these catalysts to remain stable across multiple reuse cycles highlights their robustness under varying reaction conditions. In this study, the changes in the properties of Fe/Cu and Fe/Ni BNPs before and after the reaction were analyzed, along with their potential for reuse in the HDC PCB-138 process. The assessment was conducted through an analysis of surface morphology and conversion efficiency after 5 cycles, as illustrated in Fig. 8.

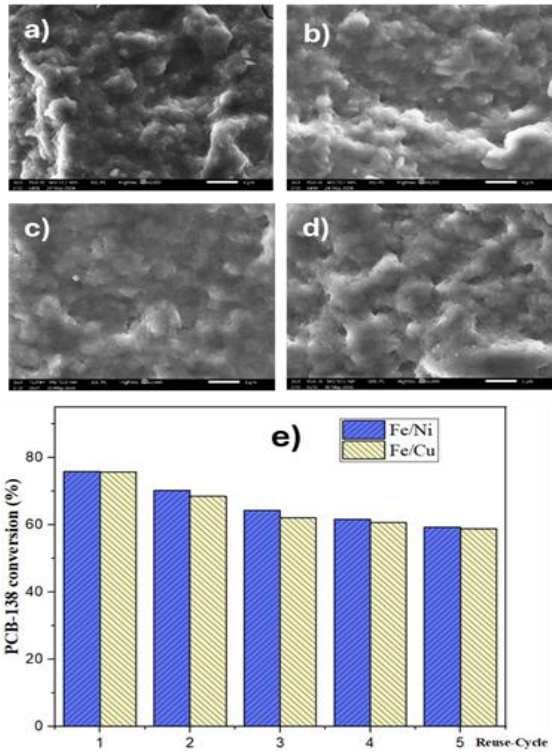

Fig. 8. a, b) SEM images of Fe/Cu before and after reaction; c, d) SEM images of Fe/Ni before and after reaction; e) Conversion efficiency of PCB-138 after 5 cycles

From the SEM images (Fig. 8a-d), it is evident that the surface morphology of the two BNPs-Fe^0 systems did not undergo significant changes after the HDC reaction. The surface structure remained stable, with no noticeable signs of severe damage. This indicates that the nanoparticles exhibit good durability during the reaction process, particularly when subjected to multiple reuse cycles. However, as observed from the PCB-138 conversion efficiency results (Fig. 8e), efficiency decreased progressively with each reuse cycle, dropping from 75.85% to 59.34% and from 75.70% to 58.93% after five cycles for Fe/Ni and Fe/Cu systems, respectively. This decline can be attributed to two primary factors: surface saturation and oxidation. The active sites on the BNPs' surface may become occupied by reaction by-products or adsorbed substances, thereby reducing catalytic efficiency. Although no significant structural degradation was observed in the SEM images, it is possible that a thin oxide layer was formed on the surface of the BNPs, which could adversely affect their reductive properties and the ability to regenerate catalytic activity. To minimize environmental concerns, BNPs should be removed from treated water immediately after reaction using simple separation methods such as membrane filtration.

4. Conclusion

In summary, BNPs-Fe^0 exhibits significant catalytic activity in the HDC reaction, with the highest transformation efficiency of PCB-138 reaching 75.70-75.85% under optimized conditions: [BNPs-Fe^0] equal 2.0 g/L, *t* equal 180 min, at *pH* value of 3 for Fe/Cu and *pH* equal 7 for Fe/Ni. These findings highlight BNPs-Fe^0 as promising candidates for large-scale environmental applications, providing a versatile and eco-friendly approach for the remediation of hazardous pollutants in contaminated water systems. The proposed transformation pathway of PCB-138 follows the sequence: PCB-138 → PCB-99 → PCB-49 → PCB-18 → PCB-4 → PCB-1 → Biphenyl.

Acknowledgments

The authors acknowledge the facilities and the scientific and technical assistance at the Institute of New Technology and Gevicat Laboratory/Hanoi University of Science and Technology.

References

[1] Behera, A., Mittu, B., Padhi, S., Patra, N., Singh, J., Chapter 25 - Bimetallic nanoparticles: green synthesis, applications, and future perspectives, in Multifunctional Hybrid Nanomaterials for Sustainable Agri-Food and Ecosystems: Micro and Nano Technologies, Elsevier, 2020, pp. 639-682. https://doi.org/10.1016/B978-0-12-821354-4.00025-X

[2] Wu, X., Guo, H., Feng, J., Zhang, L., and Liu, H., Cu/Fe Bimetallic treatment performance on organophosphorus pesticides, Frontiers in Environmental Science, vol. 10, Jun. 2022, Art. no. 915465. https://doi.org/10.3389/fenvs.2022.915465

[3] Ayoub, Ghada and Antoine Ghauch, Assessment of bimetallic and trimetallic iron-based systems for persulfate activation: application to sulfamethoxazole degradation, Chemical Engineering Journal, vol. 256, pp. 280–292, Nov. 2014. https://doi.org/10.1016/j.cej.2014.07.002

[4] Weng, X. L., Cai, W. Q., Lan, R., Sun, Q., & Xu, M. , Enhancement of catalytic degradation of amoxicillin in aqueous solution using clay supported bimetallic Fe/Ni nanoparticles, Chemosphere, vol. 103, pp. 80–85, May 2014. https://doi.org/10.1016/j.chemosphere.2013.11.033

[5] Umasangaji, H. and Y. Ramili, Status of polychlorinated biphenyl (PCBs) contamination in several marine and freshwater sediments in the world during the last three decades, IOP Conference Series: Earth and Environmental Science. vol. 584, no. 1, IOP Publishing, 2020, Art. no. 012012. https://doi.org/10.1088/1755-1315/584/1/012012

[6] Zhang, Z., Hu, S. A., Baig, S. A., Tang, J., and Xu, X., Catalytic dechlorination of Aroclor 1242 by Ni/Fe bimetallic nanoparticles, Journal of Colloid and Interface Science, vol. 385, iss. 1, pp. 160–165, Nov. 2012. https://doi.org/10.1016/j.jcis.2012.07.024

[7] M. Gil-Díaz, R. A. Pérez, J. Alonso, E. Miguel, S. Diez-Pascual, and M. C. Lobo, Iron nanoparticles to recover a co-contaminated soil with Cr and PCBs, Scientific Reports, vol. 12, iss. 1, 2022, Art. no. 3541. https://doi.org/10.1038/s41598-022-07558-w

[8] G. Tavoularis and M. A. Keane, Gas phase catalytic dehydrochlorination and hydrodechlorination of aliphatic and aromatic systems, Journal of Molecular Catalysis A: Chemical, vol. 142, pp. 187–199, Jun. 1999. https://doi.org/10.1016/S1381-1169(98)00272-6

[9] Hong Son Nguyen, Van Hoang Nguyen, Thi Thu Huong Nguyen, Ngoc Toan Vu and Ngoc Hoan Le, Optimization of Fe/Ni, Fe/Cu bimetallic nanoparticle synthesis process utilizing concentrated Camellia sinensis extract solution and activity evaluation through methylene blue removal reaction, Nano Express (IOP Publishing), vol. 5, iss. 1, Jun. 2024, Art. no. 015025. https://doi.org/10.1088/2632-959X/ad5221

[10] L. S. Balistrieri and J. W. Murray, The surface chemistry of goethite (a-FeOOH) in major ion seawater, American Journal of Science, vol. 281, iss. 6, pp. 788–806, Jun. 1981. https://doi.org/10.2475/ajs.281.6.788

[11] L. I. Osemwengie and G. W. Sovocool, The mass spectrometric ortho effect studied for all 209 PCB congeners, International Journal of Mass Spectrometry vol. 352, pp. 51–64, Oct. 2013. https://doi.org/10.1016/j.ijms.2013.07.003

[12] Shi, B., Li, C., Han, R., Li, Q., Li, P., and Chen, X, Single-step synthesis of nanocrystalline Fe-Ni/Fe-Co-Ni magnetic alloy coating via directional plasma spray, Materials, vol. 16, iss. 7, Mar. 2023, Art. no. 2544. https://doi.org/10.3390/ma16072544

[13] A. Khan, A. Rashid, R. Younas, and R. Chong, A chemical reduction approach to the synthesis of copper nanoparticles, International Nano Letters, vol. 6, no. 1, pp. 21–26, 2016. https://doi.org/10.1007/s40089-015-0163-6

[14] Venkateshaiah, A., Jayaprakash, G. K., Lee, B. K., and Kim, K. H., A comparative study of the degradation efficiency of chlorinated organic compounds by bimetallic zero-valent iron nanoparticles, Environmental Science: Water Research and Technology, vol. 8, iss. 1, pp. 162–172, 2022. https://doi.org/10.1039/D1EW00791B

[15] Patanjali Varanasi, Andres Fullana, and Sukh Sidhu, Remediation of PCB contaminated soils using iron nano-particles, Chemosphere, vol. 66, iss. 6, pp. 1031-1038, Jan. 2007. https://doi.org/10.1016/j.chemosphere.2006.07.036

[16] Zhao, M., Wu, S., Liu, H., Xu, J., and Wang, J, Modified zero-valent iron nanoparticles enhanced remediation of PCBs-contaminated soil, Science of The Total Environment, vol. 940, Aug. 2024, Art. no. 173349. https://doi.org/10.1016/j.scitotenv.2024.173349

[17] Sun, Y., Liu F., and Yang, L., Degradation of PCB67 in soil using the heterogenous Fenton process induced by montmorillonite supported nanoscale zero-valent iron, Journal of Hazardous Materials, vol. 406, Mar. 2021, Art. no. 124305. https://doi.org/10.1016/j.jhazmat.2020.124305

[18] X. Cao, H. Wang, C. Yang, L. Cheng, K. Fu, and F. Qiu, Nanoscale zero-valent iron supported on carbon nanotubes for polychlorinated biphenyls removal, Desalination and Water Treatment, vol. 201, pp. 173–186, Oct. 2020. https://doi.org/10.5004/dwt.2020.26091

[19] Gomes, H. I., Dias-Ferreira, C., and Ribeiro, A. B., Electrodialytic remediation of polychlorinated biphenyls contaminated soil with iron nanoparticles and two different surfactants, Journal of Colloid and Interface Science, vol. 433, pp. 189–195, Nov. 2014. https://doi.org/10.1016/j.jcis.2014.07.022

[20] Y. Wu, J. Zhou, Z. Wu, Q. Ye, W. Wu, X. Liu, D. He, G. Lv, and J. Zhang, Electron transfer process in dechlorination of polychlorinated biphenyls (PCBs) by nickel/zero-valent iron: Effects of temperature and selectivity pattern, Chemical Engineering Journal, vol. 470, 2023, Art. no. 144053 https://doi.org/10.1016/j.cej.2023.144053